Optimal resolutions for optical and NIR spectroscopy

S. Villanueva Jr.*[a], D.L. DePoy[a], J. L. Marshall[a]
[a]Department of Physics and Astronomy, Texas A&M University, 4242 TAMU, College Station, TX, USA 77846-4242

ABSTRACT

We study the effects of atmospheric emission lines in the night sky on spectroscopic measurements in the 0.4-2.4 μm range at resolutions $100 \leq R \leq 50000$ to determine an optimal observing resolution. We build a model of the background sky spectrum at various moon phases and calculate the fraction of pixels free of emission lines in 7 different band passes while varying the resolution. We then discuss the effect of the background emission on the signal-to-noise of constant flux targets to determine an optimal resolution at which to observe. Preliminary results show that the emission lines have little to no effect on the selection of resolution in the optical, but that in the wavelengths ranging from 1.0-2.4 μm the effects of atmospheric emission line suggests observing at a resolution of $R>2000$ is recommended.

Keywords: Emission lines, spectroscopy, atmosphere, emission, continuum, optimal, resolution

1. INTRODUCTION

This study builds upon previous works by Martini and DePoy[1] concerning the effect of OH airglow emission lines on ground-based near-infrared spectroscopy with a goal to expand by including optical wavelengths and various continuum values based on moon phases. The purpose of this work is to determine the effect of the dominant source of background noise, the atmospheric emission lines, in optical and near-infrared spectroscopic observations at various dispersions from 0.4-2.4 μm over the 7 different band passes as shown in Table 1. Although the resolution of each spectroscopic observation will ultimately be determined by the science goals behind the observation we attempt to provide as much input into the decision making process as possible. We discuss the creation of the sky emission models, the data sets used to calculate the background noise, the fraction of pixels contaminated by emission lines, signal-to-noise ratio (SNR) calculations, and results.

Table 1. The seven wavelength ranges and corresponding filter names used as references in this study.

Filter	Wavelength [μm]
U	0.30-0.40
B	0.40-0.50
V	0.50-0.60
R	0.60-0.72
I	0.72-1.00
J	1.16-1.34
H	1.50-1.80
K	2.00-2.40

*svillan@neo.tamu.edu

Ground-based and Airborne Instrumentation for Astronomy IV, edited by Ian S. McLean, Suzanne K. Ramsay, Hideki Takami, Proc. of SPIE Vol. 8446, 84462V · © 2012 SPIE · CCC code: 0277-786X/12/$18 · doi: 10.1117/12.926505

2. BACKGROUND MODEL

2.1 Constructing the sky emission spectra

We make use of publicly available data online at the European Southern Observatory's (ESO) E-ELT Design Reference Mission website[2] to build our atmospheric emission model at high resolutions. For our study, the background flux f_{BKG} is modeled on three components: continuum, atmospheric emission, and individual emission lines. Each component is contained in separate data files, modeled individually, and then added together:

$$f_{BKG}(\lambda) = cont(\lambda) + atm(\lambda) + em.lines(\lambda). \quad (1)$$

The atmospheric component is taken from ESO data files[3] with fluxes given in a dispersion of $\Delta\lambda_D$=2.0x10^{-6} μm. This sampling is used as the base for all later dispersions and resolutions. All lower dispersions are binned in multiples of $\Delta\lambda_D$=2.0x10^{-6} μm.

2.2 Continuum

The continuum is attributed to diffuse galactic emission, zodiacal light, and moonlight. The values for the continuum evolve with moon phase and vary as the moon transitions from 0-14 days from new moon. The continuum values for the B, V, R, and I bands are taken from the standard ESO ETC sky brightness table[4]. The continuum values for the J, H, and K bands are taken to be constant with moon phase[2]. A summary of the ESO values used in our calculations are given in Table 2.

Table 2. Continuum brightness for the various filter ranges and moon phases as summarized from the ESO tables. J, H, and K band fluxes are assumed constant with moon phase.

Continuum brightness [photons/s/m^2/μm/arcsec^2]					
Filter	**Days from new moon**				
	0	**3**	**7**	**10**	**14**
U	120	190	830	3000	12000
B	110	150	310	720	2200
V	190	210	280	530	1000
R	310	340	410	540	780
I	500	500	600	720	950
J	1200	1200	1200	1200	1200
H	2300	2300	2300	2300	2300
K	2300	2300	2300	2300	2300

Instead of using the continuum data from ESO to create a continuum that appears as a step function we create a continuous function by fitting a cubic spline to the midpoints of the filter ranges in Table 1 with the continuum values in Table 2. This serves to give the continuum a more natural shape akin to the background model used by Gemini[5]. A comparison of the ESO model and the fit we use can be seen in Figure 1. The ESO data files are preferred to the Gemini model as they are available at higher resolutions that can be binned down at our convenience.

2.3 Emission lines

The list of emission lines is also taken from ESO each are contained in separate files for the optical and near-infrared[6]. For each of the emission lines we assume a Gaussian profile with a full-width-at-half-maximum (FWHM) set to twice the dispersion or FWHM=2$\Delta\lambda_D$. The FWHM is used as the $\Delta\lambda_R$=2$\Delta\lambda_D$ when calculating the resolution R=$\lambda/\Delta\lambda_R$. For the

remainder of the paper we will commonly refer to the resolution instead of the dispersion. To create the Gaussian profile for each emission line the integrated line flux $\int flux_i$ is transformed into the form

$$f_i(\lambda) = a_i e^{\frac{-(x-\lambda_i)^2}{2c^2}} \tag{2}$$

by the following process:

$$FWHM = 2\Delta\lambda_D = 2\sqrt{2\ln 2}\, c \tag{3}$$

$$c = \frac{\Delta\lambda_D}{\sqrt{2\ln 2}} \tag{4}$$

$$\int_{-\infty}^{+\infty} a_i e^{\frac{-(x-\lambda_i)^2}{2c^2}} d\lambda = a_i c\sqrt{2\pi} = \int flux_i \tag{5}$$

$$a_i = \frac{\int flux_i}{c\sqrt{2\pi}}. \tag{6}$$

This gives all of the necessary terms in Eq. 2 to create the individual emission lines at each wavelength λ_i. The c term is calculated based on the dispersion of each spectra and is also used to find the scale factor a_i. We assume a strict Gaussian form for each emission line and do not include any contributions from other sources that may cause line broadening beyond the Gaussian profile.

2.4 Compiling the spectra

Beginning with the initial dispersion $\Delta\lambda_D$=2.0x10^{-6} μm each emission line is converted into a Gaussian profile. The flux of each $\Delta\lambda_D$ bin in the atmospheric file is added to the cubic spline continuum flux in each wavelength bin. Next the flux of all emission lines within 6 standard deviations of the wavelength bin is added into the total flux. At more than a few standard deviations the emission line flux is nearly zero and this cutoff greatly decreases the time required to build each spectra. This process is then repeated for multiples of $\Delta\lambda_D$ in three different samplings. The highest resolutions are done for $\Delta\lambda_D$=2.0x10^{-6} μm to $\Delta\lambda_D$=2.0x10^{-4} μm sampled at every 2.0x10^{-6} μm. The medium resolutions use $\Delta\lambda_D$=2.0x10^{-4} μm to $\Delta\lambda_D$=2.0x10^{-3} μm at every $\Delta\lambda_D$=2.0x10^{-5} μm and the lowest resolutions sample from $\Delta\lambda_D$=2.0x10^{-5} μm to $\Delta\lambda_D$=2.0x10^{-2} μm at every $\Delta\lambda_D$=1.0x10^{-3} μm.

An example of the finished spectra with all 5 moon phases from §2.2 is shown in Figure 2. Because the continuum is assumed constant over most of the wavelengths the new moon continuum values are used for simplicity. Examples of low and high resolution spectra can be seen in the upper halves of Figures 3-5 with each showing selected wavelength ranges.

3. CONTAMINATED PIXELS

3.1 Contaminated pixels metric

Once all of the spectra have been built we wish to evaluate what fraction of pixels in each filter band pass has emission line contamination. To do this each pixel or $\Delta\lambda_D$ element must be evaluated by some metric. We use the following contamination ratio to determine if a pixel element meets this metric:

$$\frac{\sqrt{continuum}}{\sqrt{continuum+emission\ lines+atmospheric}}. \tag{7}$$

This is used to judge whether a pixel is contaminated due to the emission lines and thermal atmospheric component relative to the continuum. This is a measure of the degree that the emission lines and thermal atmospheric emission comprises the SNR of a sky limited observation. This metric is most sensitive to the emission lines in the longer wavelengths where the emission lines contain orders of magnitude more flux than the continuum and this is typically not the case in the optical. This causes the value of the metric to become very small when emission lines are present and

when the value falls to less than 0.8 each pixel is flagged as contaminated. The value from this metric for each pixel is shown just below the low and high resolution spectra in Figures 3-5.

3.2 Uncontaminated pixel fraction

Using this metric we evaluate the evolution of free pixels versus resolution as shown in Figure 6. In the B, V, and R bands there is a low fraction of contaminated pixels at nearly all resolutions. Although there are emission lines in these wavelength ranges they are not very dense and they have small fluxes relative to the continuum. In the B band the continuum tends to dominate at low resolutions resulting in some emission lines no longer being able to flag a pixel as contaminated. This results in an increase in the number of uncontaminated pixels at low resolutions according to our metric. In the I, J, H, and K bands the strengths of the emission lines are much greater and occur more frequently. The Gaussian wings of the emission lines overlap at lower resolutions in these band passes which results in over half of the pixels meeting the contaminated pixel requirement at resolutions R<1000. The most drastic example occurs in the H band where over 90% of the pixels are contaminated at resolutions R<1000.

Table 3. Values used in the SNR calculations.

Parameter	Name	Value	Units
f_{obj}	Object flux	See §4.2	$\gamma\ s^{-1}\ m^{-2}\ \mu m^{-1}$
t_{int}	Integration time	600	s
D_T	Mirror diameter	8.4	m
A_T	Mirror area	221.7	m^2
$\Delta\lambda_D$	Pixel size	See §2.4	μm
η	System throughput	0.5	*electrons* γ^{-1}
f_{bkg}	Background flux	See §2.4	$\gamma\ s^{-1}\ m^{-2}\ \mu m^{-1}\ arcsec^{-2}$
$d\Omega$	Slit area	0.08	$arcsec^{-2}$
D	Dark current	0.05	*electrons* s^{-1}
N_R	Read noise	5.0	*electrons*

4. SIGNAL-TO-NOISE (SNR)

4.1 The SNR expression

To calculate the effect of the background flux on optical and near infrared observations we prefer to look at the SNR in each pixel. We use the standard SNR expression:

$$SNR = \frac{N_S}{\sqrt{N_S+N_B+N_D+N_R^2}}. \quad (8)$$

Here, N_S, N_B, N_D, and N_R, are the signal in electrons from the source, background, detector, and read noise. Or in detail, the expressions are given as:

$$N_S = f_{obj} t_{int} A_T \Delta\lambda_D \eta \quad (9)$$

$$N_B = f_{bkg} t_{int} A_T \Delta\lambda_D d\Omega \eta \quad (10)$$

$$N_D = D t_{int}. \quad (11)$$

To maintain continuity with the previous works we adopt the same values used by Martini and DePoy[1]. The names and values are listed in Table 3. These values are based on a large 8.4 meter telescope capable of observing 20th magnitude objects in the 0.4-2.4 μm range with a resolution 100≤R≤50000.

4.2 Signal-to-noise versus resolution

To quantify the effects of the background continuum and emission lines in each pixel element we calculate the SNR. To do this we create seven 20th magnitude test objects with constant fluxes in each pixel within each filter band pass. The SNR is calculated according to §4.1 in each pixel element at each $\Delta\lambda_D$ described in §2.4. After calculating the SNR in each band pass the individual SNR values are ranked from highest to lowest. The SNR at the 10th, 25th, 50th, and 75th percentiles are then plotted against resolution in Figures 7-10. In the limit that there is no background noise and the signal is dominated by the object flux one would expect the SNR to decrease as one approaches higher resolutions in each pixel. This decrease in SNR is the result of spreading the finite object flux over an increasing number of pixels with constant read noise and dark current. In this limit going to lower resolutions results in increased SNR at the loss of spectral resolution.

This is the trend in the B, V, and R bands where the emission lines and the background flux are weak relative to the 20th magnitude object flux. There is a slight divergence from this curve in the I band where the emission lines begin to contribute. The effect is more noticeable in the J and K bands where the SNR begins to decrease in over half the pixels at resolutions R<2000. In these two bands there is a slight peak in the curves. This implies that going to lower resolutions will not result in higher SNR.

The H band has the most pronounced decrease in SNR with 90 percent of the pixels losing SNR at resolutions R<1000. At least half of the pixels' SNR begin to decrease for R<3000 and a quarter of the pixels lose SNR for R<10000.

5. CONCLUSIONS

After creating a model of the background sky in the 0.4-2.4 μm range we find that over half of the pixels meet our metric as being contaminated by emission line flux at resolutions R<1000 in the I, J, H, and K bands. At shorter optical wavelengths the strength and density of atmospheric emission lines has little to no effect on the SNR that is dominated by the continuum. At longer wavelengths the stronger more frequent emission lines begin to reduce the SNR even at lower resolutions where greater SNR is expected. This causes a peak in the SNR at resolutions R~2000 in the J and K bands indicating that at lower resolutions no signal is gained even while decreasing the spectral resolution. The H band is the most problematic with over half the pixels losing SNR and spectral resolution for R<3000.

Most observers will want to strike a balance between maximizing the SNR and maximizing spectral resolution during spectroscopic observations, but we show that neither is gained by observing at resolutions below ~2000 in the J, H, and K bands. While individual science goals will determine the resolution of most observations our results suggest that a resolution R>2000 should be used while observing in the 1.0-2.4 μm range.

ACKNOWLEDGMENTS

Texas A&M University thanks Charles R. '62 and Judith G. Munnerlyn, George P. '40 and Cynthia Woods Mitchell, and their families for support of astronomical instrumentation activities in the Department of Physics and Astronomy.

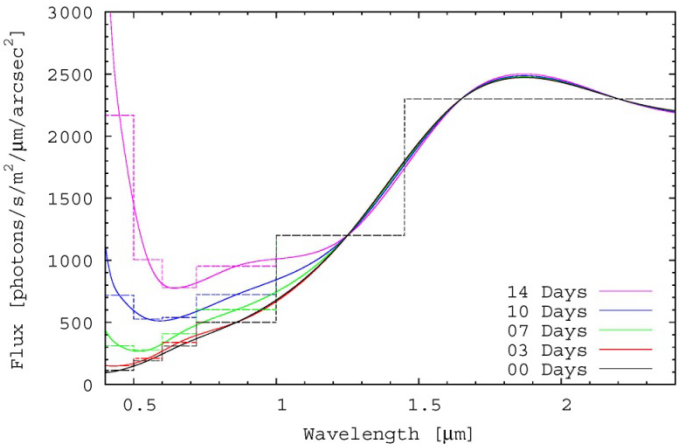

Figure 1. The background sky continuum flux as a function of wavelength. The ESO values appear as step functions and are shown in the dashed lines with the cubic spline fits shown in solid lines. The continuum is dependent on moon phase in the optical, but is assumed constant in the J, H, and K bands.

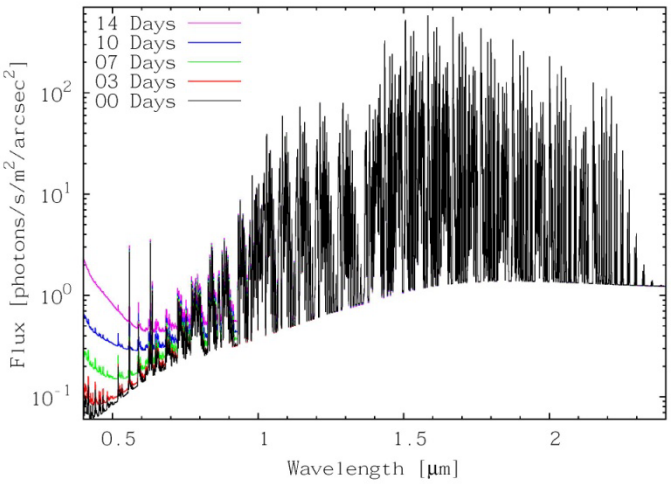

Figure 2. Compiled background model from 0.4-2.4µm complete with Gaussian emission lines. The continuum for each of the 5 moon phases is shown and the models appear very similar at longer wavelengths due to the assumed constant continuum. For simplicity the continuum at new moon is used throughout the paper.

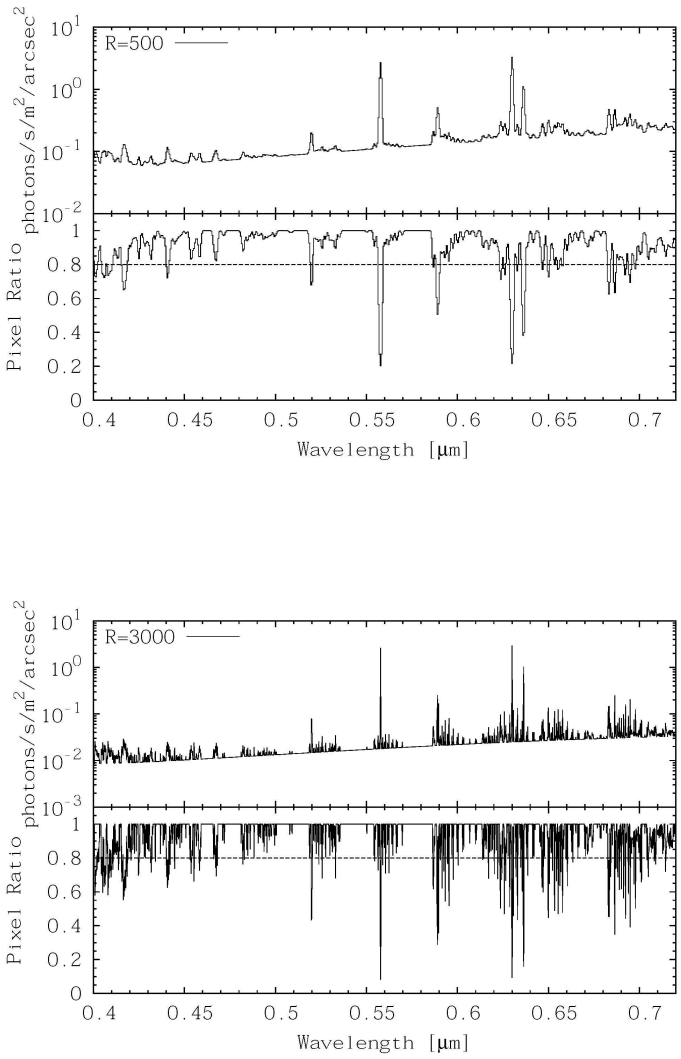

Figure 3. Examples of low and high resolution spectra in the B, V, and R band wavelength ranges. The flux of each wavelength bin is shown above with the corresponding value for the contaminated pixel metric as detailed in §3.1. In the optical bands the number of free pixels remains roughly constant over all resolutions.

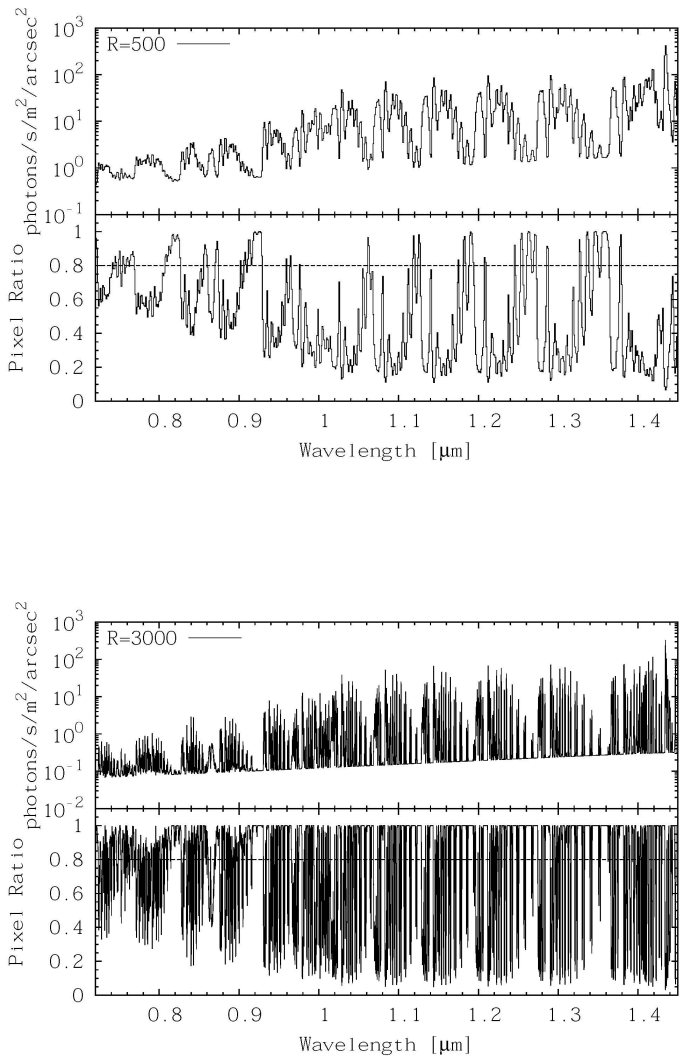

Figure 4. Examples of low and high resolution spectra in the I and J band wavelength ranges. The flux of each wavelength bin is shown above with the corresponding value for the contaminated pixel metric as detailed in §3.1. The strength and density of the emission lines begins to increase over these wavelengths. There is a noticeable difference in the number of uncontaminated pixels in the low resolution panel.

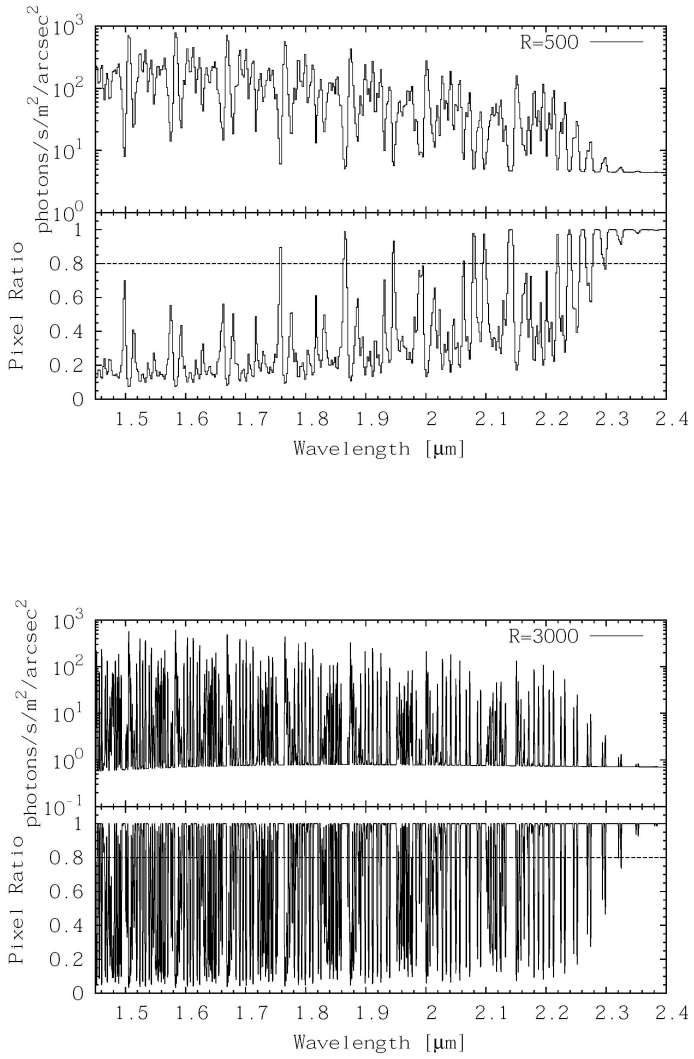

Figure 5. Examples of low and high resolution spectra in the H and K band wavelength ranges. The flux of each wavelength bin is shown above with the corresponding value for the contaminated pixel metric as detailed in §3.1. The strength and density of the emission lines dominate in the H band (1.5-1.8μm) where there is only one pixel that meets the uncontaminated pixel metric. The H band has a decreased number of emission lines beyond 2.3 μm that helps increase the fraction of uncontaminated pixels in that range.

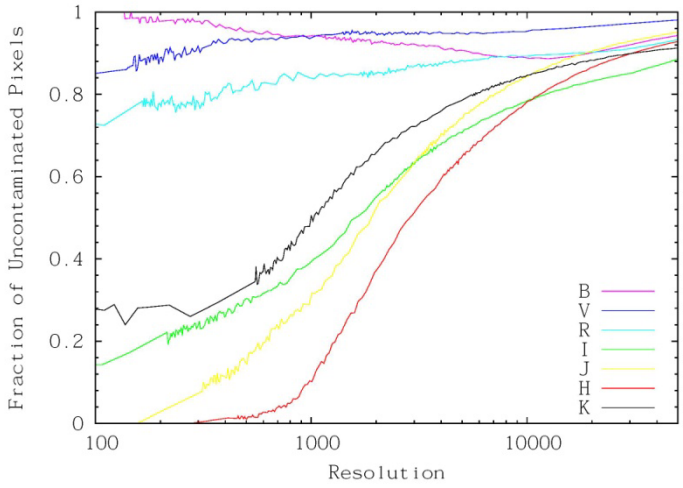

Figure 6. The fraction of uncontaminated pixels versus resolution. At resolutions lower than 1000 at least half of the pixels in the I, J, H, and K bands are contaminated with the H band having less than 10% free. The B, V, and R bands remain fairly uncontaminated at all wavelengths. Because of the low flux and low number of emission lines in the B band the continuum begins to dominate at low resolutions resulting in the pixels becoming uncontaminated.

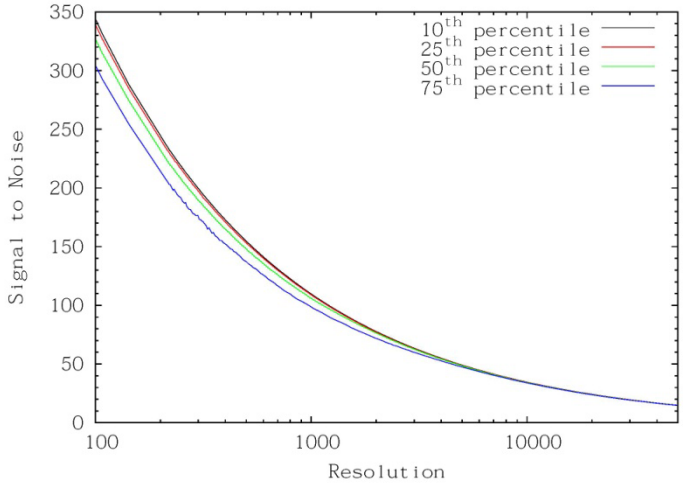

Figure 7. I band signal-to-noise at various resolutions. The SNR is rank ordered and the 10th, 25th, 50th, and 75th percentile curves are shown. The emission lines cause little divergence from an emission line free curve. The four curves are indistinguishable in the B, V, and R bands.

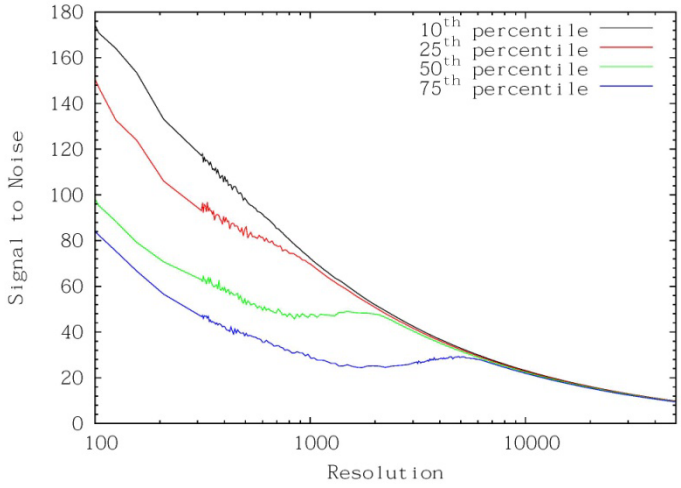

Figure 8. J band signal-to-noise at various resolutions. The SNR is ranked and the 10th, 25th, 50th, and 75th percentile curves are shown. At least half of the pixels' SNR begin to decrease for R<2000 with a quarter of the pixels losing SNR for R<5000.

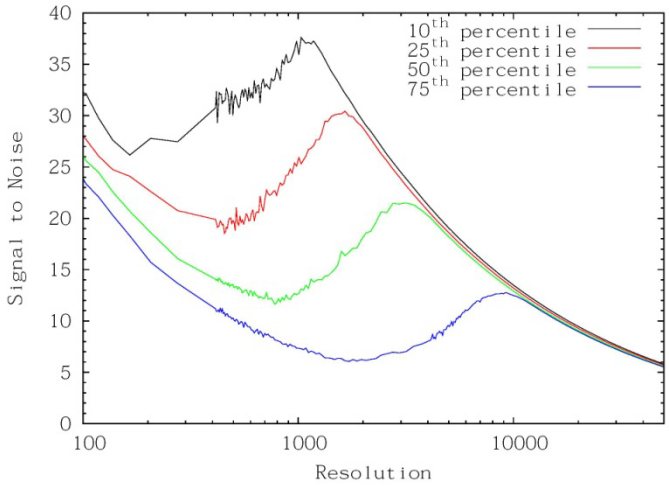

Figure 9. H band signal-to-noise at various resolutions. The SNR is ranked and the 10th, 25th, 50th, and 75th percentile curves are shown. The H band has the most pronounced decrease in SNR at low resolution with 90 percent of the pixels are losing SNR at resolutions R<1000. At least half of the pixels' SNR begin to decrease for R<3000 with a quarter of the pixels losing SNR at R<10000.

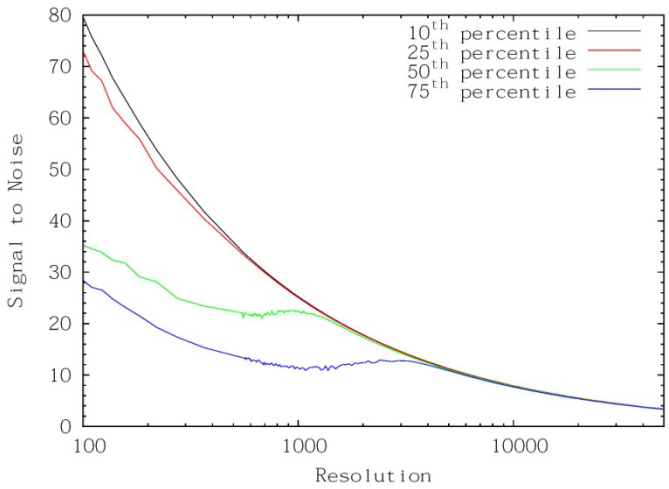

Figure 10. K band signal-to-noise at various resolutions. The SNR is ranked and the 10^{th}, 25^{th}, 50^{th}, and 75^{th} percentile curves are shown. The K band is almost entirely free of emission lines above 2.3 μm resulting in the 10^{th} and 25^{th} percentile curves appearing very similar to those in the I and J band. The rest of the K band is more similar to the H band and at least half of the pixels' SNR begin to decrease for R<1000 with a quarter of the pixels losing SNR for R<3000.

REFERENCES

[1] Paul Martini and D. L. DePoy, 2000 Proceedings of the SPIE, Vol. 4008, 695
[2] <http://www.eso.org/sci/facilities/eelt/science/drm/tech_data/background/>
[3] <http://www.eso.org/sci/facilities/eelt/science/drm/tech_data/data/atm_em/>
[4] <http://www.eso.org/observing/etc/doc/gen/formulaBook/node20.html>
[5] <http://www.gemini.edu/sciops/telescopes-and-sites/observing-condition-constraints/optical-sky-background>
[6] <http://www.eso.org/sci/facilities/eelt/science/drm/tech_data/data/optical_ir_sky_lines.dat>